Supporting Information for

Rigidity-Flexibility Balance Strategy Enables Highly photoluminescent Two-dimensional Covalent Organic Framework Nanosheets

Hao Wang,[a‡] Chengtao Gong,[a‡] Peng Jin,[a] Chenglong Guo,[a] Danfeng Wang,[a] Guodong Xu,[b] and Yongwu Peng*[a]

[a]College of Materials Science and Engineering and College of Chemical Engineering, Zhejiang University of Technology, Hangzhou, 310014, China

[b]Jiangsu Province Engineering Research Centre of Agricultural Breeding Pollution Con-trol and Resource, Yancheng Teachers University, Yancheng 224007, China

E-mail: ywpeng@zjut.edu.cn

‡H Wang and G. T. Gong contributed equally to this work.

Table of Content

1. Materials and methods…….. S3
2. Synthesis and general procedures……. S5
2.1. Synthesis of monomers…….. S5
Figure S1. ^{1}H NMR spectra…… S6
Figure S2. ^{13}C NMR spectra…… S6
Figure S3. HRMS spectra…… S7
2.2. Synthesis and characterization of COFs…… S8
Figure S4. FT-TR spectra…… S9
Figure S5. ^{13}C CP/MAS NMR spectra…… S9
Figure S6. TGA curves……... S10
Figure S7. PXRD patterns with different stacking models…… S10
Figure S8. Enlarged experimental and simulated PXRD patterns……S10
Figure S9. SEM images…… S11
Figure S10. TEM images…… S11
Figure S11. AFM image and layer distance …… S12
2.3. Fluorescence detection performance
Figure S12. Photoluminescence images…... S12
Figure S13. CIE chromaticity diagram…… S13
Figures S14-16. Fluorescence quenching experiments…….. S13
Figure S17. Mechanism study for fluorescence quenching experiments……S15
Figure S18. Recycle, specificity, and anti-interference experiments…..……S15
2.4. Unit cell parameters and fractional atomic coordinates…….. S16
Table S1-2. Unit cell parameters and fractional atomic coordinates…… S16
2.5. Quantum yield (PLQY) data of reported fluorescent COFs…… S19
Table S3. Comparative table for quantum yield (PLQY) data of reported fluorescent COFs…..……...
S19
3. References…… S21

1. Materials and methods

All the chemicals are commercially available, and used without further purification. All solvents were dried and distilled according to conventional methods.

Power X-ray diffraction (PXRD): PXRD patterns were collected on an X-ray diffraction (XRD) system (DX-27mini, China) using Cu Kα radiation.

Fourier transform infrared (FT-IR): IR spectrum was measured on an IR spectrometer (Nicolet 6700) between the ranges of 4000 to 400 cm^{-1}.

Solution nuclear magnetic resonance (NMR): Liquid state ^{1}H nuclear magnetic resonance spectroscopy was collected on a Varian Mercury Plus 400 NMR Spectrometer. Liquid State ^{13}C nuclear magnetic resonance spectroscopy was collected on a Bruker Ascend™ 400 MHz NMR Spectrometer.

High resolution mass spectrometry (HRMS): The electrospray ionization mass spectrometry (ESI-MS) spectra were recorded using an Sciex X500R QTOF MS spectrometer.

Solid-state nuclear magnetic resonance (ssNMR): Solid-state nuclear magnetic resonance (NMR) data were performed on a Bruker AVANCE III 600 spectrometer with cross-polarization magic-angle-spinning (CP/MAS) at a resonance frequency of 150.9 MHz. ^{13}C CP/MAS NMR spectra were recorded using a 4 mm MAS probe and a spinning rate of 12kHz. A contact time of 4 ms and a recycle delay of 2 s were used for the ^{13}C CP/MAS NMR measurement. The chemical shifts of ^{13}C were externally referenced to tetramethylsilane (TMS).

Elemental analyses (EA): Elemental analyses were performed on an Elementar vario MICRO UNICUBE series CHN elemental analyzer.

Scanning electron microscope (SEM): SEM images were collected using a GeminiSEM 500 system.

Transmission electron microscope (TEM): TEM images were obtained with a Tecnai G2 F30 S-Twin.

Thermogravimetric analysis (TGA): TGA was performed using a TA Q5000 under flowing N_2 with 20 K min^{-1} ramp rate. Samples were heated in a Platinum pan (700 °C, 20 °C min^{-1}) under a N_2 flux (25 mL min^{-1}).

Atomic force microscopy (AFM): AFM image were recorded using a Bruker Dimension Edge AFM in tapping mode and processed by Nanoscope Analysis.

Fluorescence Spectra and Quantum Yield: Fluorescence spectra were recorded with a Hitachi F-4600 fluorescence spectrophotometer. The fluorescence quantum yield was measured with an Absolute PL quantum Yield Spectrometer QY C11347-01 ,02.

Crystal structure modeling：Structural modeling of COFs was generated using the Materials Studio[S1] program employing the *Building* (*Crystal*) module, the lattice model was geometrically optimized using force-filed based method (*Forcite* molecular dynamics module) and SCC-DFTB (*DFTB* + module). The Pawley fitting (*Reflex* module) was performed to optimize the lattice parameters iteratively until the Rwp value converges and the overlay of the observed with refined profiles shows good agreement. Powder indexing and Rietveld refinement were performed using EXPO2014[S2] various topology structures were illustrated by VESTA software [S3].

Fluorescence detection: In a typical experimental setup, 1 mg of TPE-DBC-COF nanosheets were sonicated and dispersed in 2 mL of acetone. Then 20 μL of tetracycline hydrochloride solution with gradient concentration (n mM) were added. Fluorescence (FL) spectra of the mixed solutions with $nx10^{-2}$ mM concentration of tetracycline hydrochloride were then collected using with a Hitachi F-4600 fluorescence spectrophotometer with excitation wavelength of 365 nm and emission slit of 5 nm. All detective experiments were performed 3 times and reported consistent results.

The fluorescence detection of chloramphenicol and carbamazepine using TPE-DBC-COF nanosheets were performed under the same protocol except the chloramphenicol and carbamazepine were dissolved in acetone.

2. Synthesis and general procedures

2.1 Synthesis of monomers

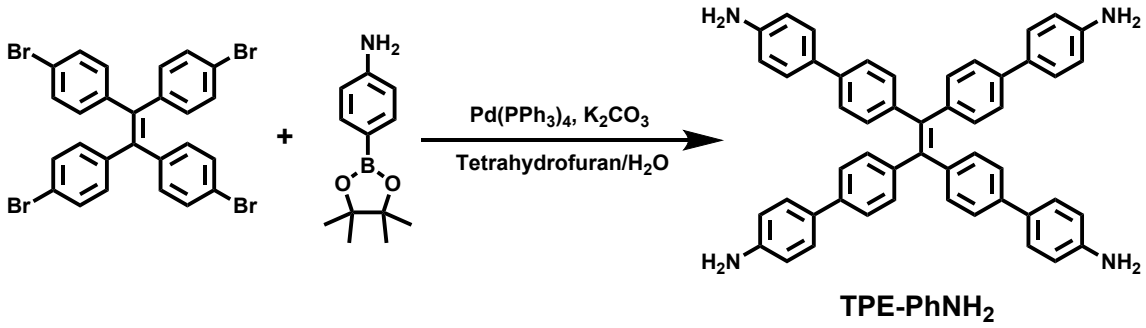

Scheme S1. 4',4''',4''''',4'''''''-(ethene-1,1,2,2-tetrayl)tetrakis(([1,1'-biphenyl]-4-amine)) (**TPE-PhNH$_2$**).

4',4''',4''''',4'''''''-(ethene-1,1,2,2-tetrayl)tetrakis(([1,1'-biphenyl]-4-amine)) (**TPE-PhNH$_2$**) was synthesized according to a previously published procedure.[S4] 1,1,2,2-tetrakis(4-bromophenyl)ethene (1.00 g, 1.55 mmol), 4-aminophenylboronic acid pinacol ester (2.72 g, 12.4 mmol), K_2CO_3 (2.57 g, 18.60 mmol), and $Pd(PPh_3)_4$ (0.18 g, 0.16 mmol) were mixed in a 250 mL single neck flask, then Tetrahydrofuran (120 mL) and H_2O (40 mL) were added. The mixture was heated at 80 ℃ for 24 h under nitrogen atmosphere and then cooled to room temperature, followed by extraction with dicholomethane. After the organic phase was washed with brine and dried over $MgSO_4$, the organic solvent was removed under reduced pressure. **TPE-PhNH$_2$** was purified by column chromatography (EA/petroleum ether, 2/1) and obtained as a yellow solid (0.61 g, yield: 57 %).

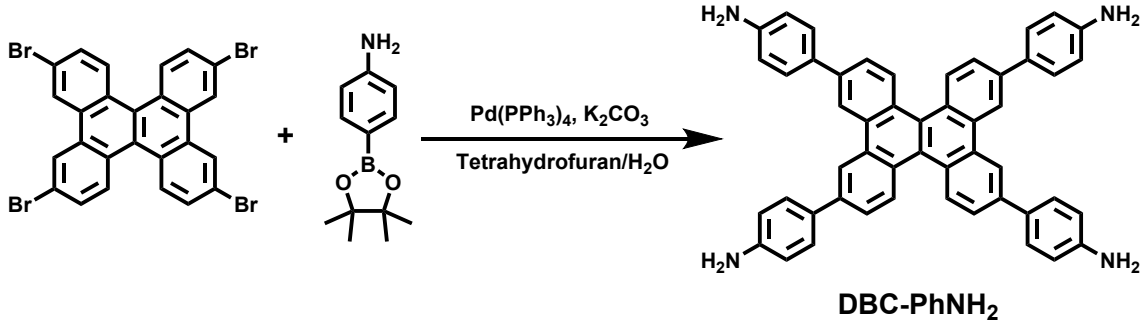

Scheme S2. 4,4',4'',4'''-(dibenzo[g,p]chrysene-2,7,10,15-tetrayl)tetraaniline (**DBC-PhNH$_2$**).

4,4',4'',4'''-(dibenzo[g,p]chrysene-2,7,10,15-tetrayl)tetraaniline (**DBC-PhNH$_2$**) was conducted vis the Suzuki reaction. 2,7,10,15-tetrabromodibenzo[g,p]chrysene (1.00g, 1.56 mmol), 4-aminophenylboronic acid pinacol ester (2.72 g, 12.4 mmol), K_2CO_3 (2.57 g, 18.6 mmol), and $Pd(PPh_3)_4$ (0.18 g, 0.16 mmol) were mixed in a 250 mL single neck flask, then Tetrahydrofuran (120 mL) and H_2O (40 mL) were added. The mixture was heated at 80 ℃ for 24 h under nitrogen atmosphere and then cooled to room temperature, followed by extraction with dicholomethane. After the organic phase was washed with brine and dried over $MgSO_4$, the organic solvent was removed under reduced pressure. **DCB-PhNH$_2$** was purified by column chromatography (dicholomethane/methanol, 20/1) and obtained as a yellow solid (0.53 g, yield: 49.1%).^{1}H NMR (400 MHz, DMSO-d^6): δ 8.98 (s, 4H), 8.61 (d, 4H), 7.91 (d, 4H), 7.72 (d, 8H), 6.71 (d, 8H), 5.31 (s, 8H).

^{13}C NMR (400 MHz, DMSO-d^6): δ 149.17, 139.38, 131.30, 129.25, 128.35, 127.44, 127.14. 126.34, 125.28, 120.24, 114.78. HRMS (ESI+): m/z: Calcd for [$C_{50}H_{36}N_4$+1H$^+$]: 693.2940, found 693.2999.

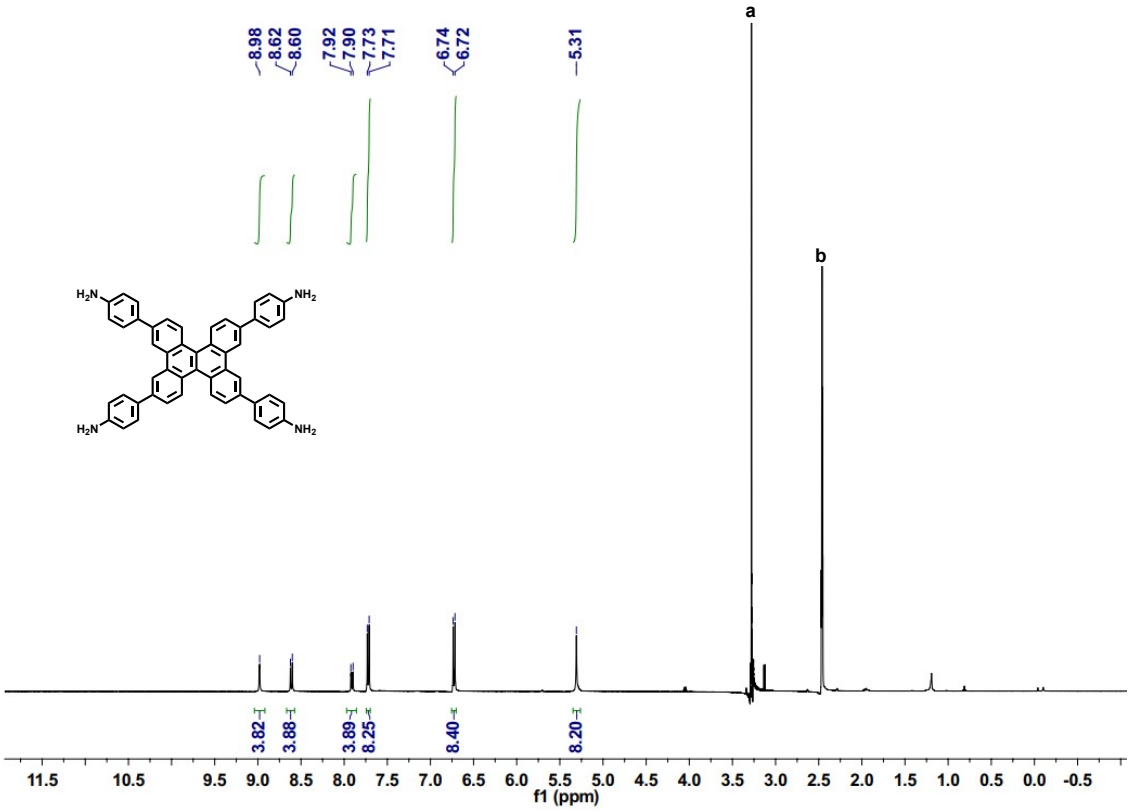

Figure S1. ^{1}H NMR spectra of **DBC-PhNH$_2$**. Solvent peaks of H_2O (a), DMSO (b).

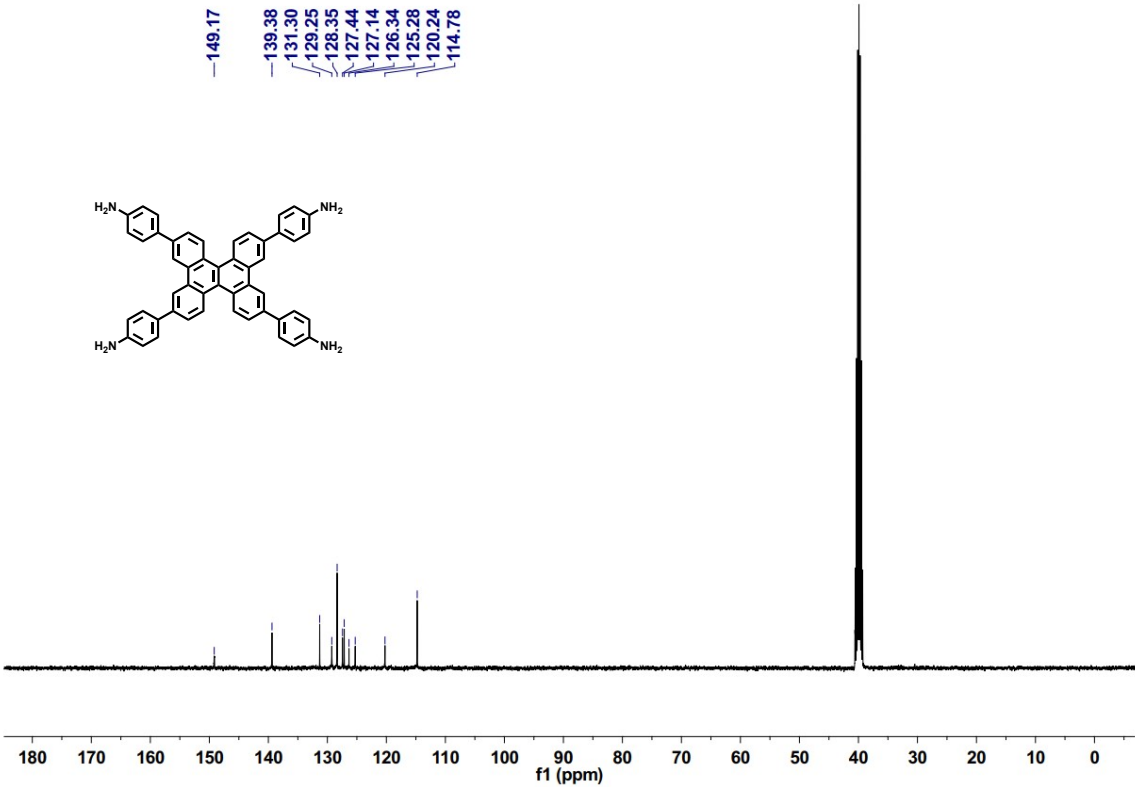

Figure S2. ^{13}C NMR spectra of **DBC-PhNH$_2$**.

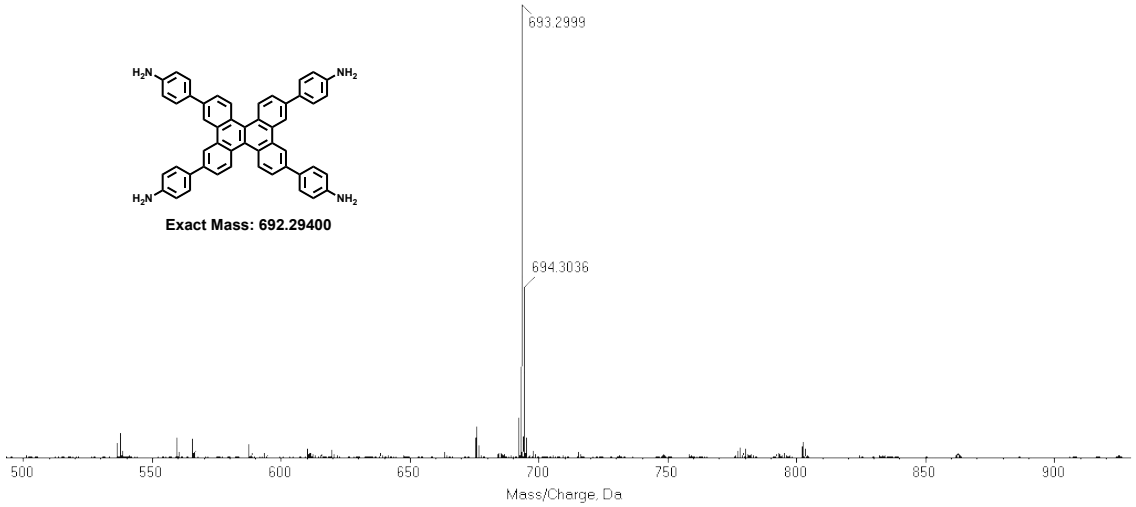

Figure S3. HRMS spectra of **DBC-PhNH$_2$**.

2.2 Synthesis and characterization of COFs

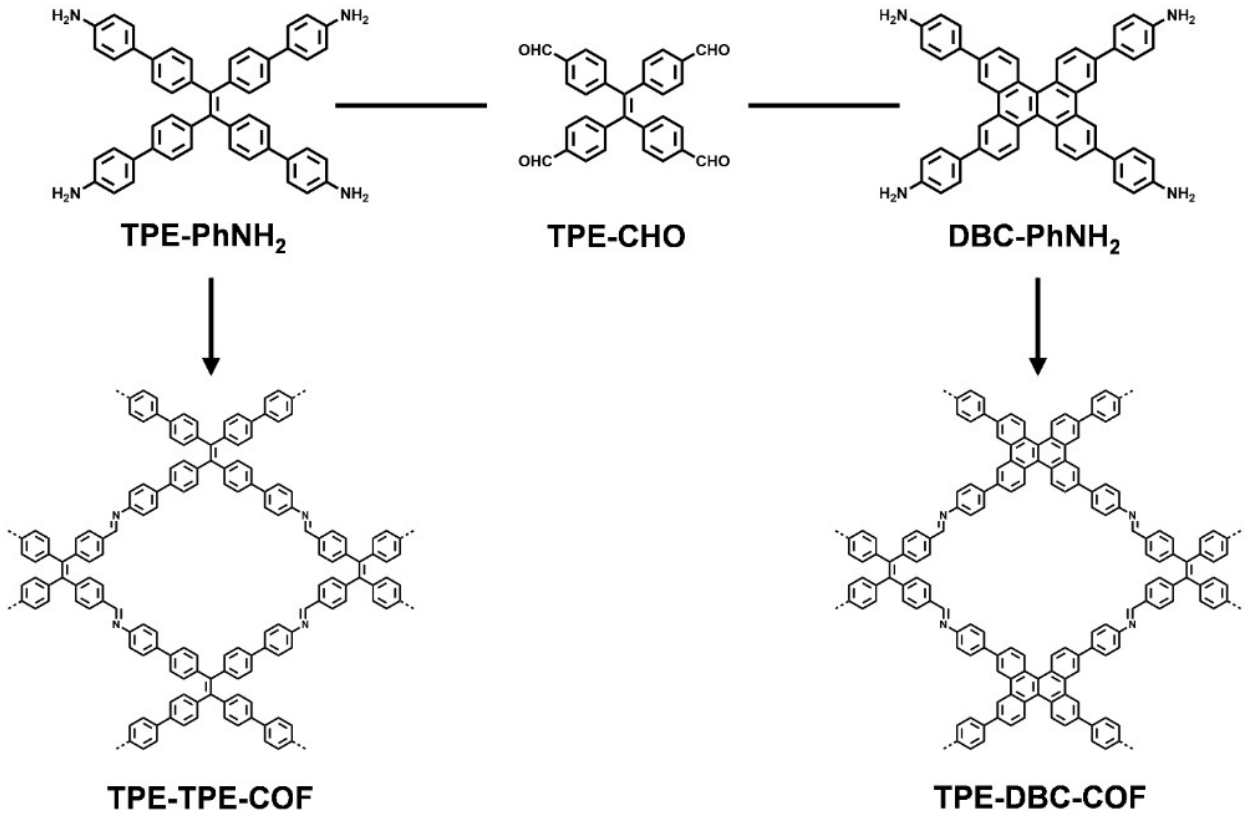

TPE-TPE-COF: TPE-PhNH$_2$ (27.9 mg, 0.04 mmol) and **TPE-CHO** (17.8 mg, 0.04mmol) were added into a glass ampoule with Mesitylene (0.6 mL) and Dioxane (0.6mL). The solution was sonicated for 5 minutes to obtain light yellow turbid solution. 6 M acetic acid (0.6mL) were added into the glass ampoule as catalyst. The glass ampoule was flash frozen at 77 K using the liquid nitrogen bath and degassed by freeze-pump-thaw three times, and then sealed. The glass ampoule was placed in an oven at 120 ℃ for 4 days. The yellow solid was isolated by centrifugation and washed with N, N-dimethylacetamide (3×10 mL) and acetone (3×10 mL). The resulting precipitate was filtered then exhaustively washed with tetrahydrofuran and acetone by Soxhlet extraction for 48 hours. The sample was then transferred to vacuum chamber and evacuated to 20 mTorr at 80 ℃ for 24 h, yielding yellow powder TPE-TPE-COF (Yield: 40.73 mg, 90.5%). Elemental analysis of TPE-TPE-COF with a molecular formula of $(C_{80}H_{52}N_4)_n$ (% Calc/Found: C 89.89/89.73, H 4.87/4.91, N 5.24/5.36).

TPE-DCB-COF: DCB-PhNH$_2$ (27.71mg, 0.04 mmol) and **TPE-CHO** (17.8 mg, 0.04mmol) were weighed into a glass ampoule with Mesitylene (0.6 mL) and Dioxane (0.6mL). The solution was sonicated for 5 minutes to obtain light yellow turbid solution. 6 M acetic acid (0.2 mL) was added into the glass ampoule as catalyst. The glass ampoule was flash frozen at 77 K using the liquid nitrogen bath and degassed by freeze-pump-thaw three times, and then sealed. The glass ampoule was placed in an oven at 120 ℃ for 4 days. The yellow solid was isolated by centrifugation and washed with N, N-dimethylacetamide (3×10 mL) and acetone (3×10 mL). The resulting precipitate was filtered then exhaustively washed with tetrahydrofuran and acetone by Soxhlet extraction for 48 hours. The sample was then transferred to vacuum chamber and evacuated to 20 mTorr at 80 ℃ for

24 h, yielding yellow powder TPE-DCB-COF (Yield: 38.65 mg, 86.3%). Elemental analysis of TPE-DCB-COF with a molecular formula of $(C_{80}H_{48}N_4)_n$ (% Calc/Found: C 90.23/90.33, H 4.51/4.27, N 5.26/5.40).

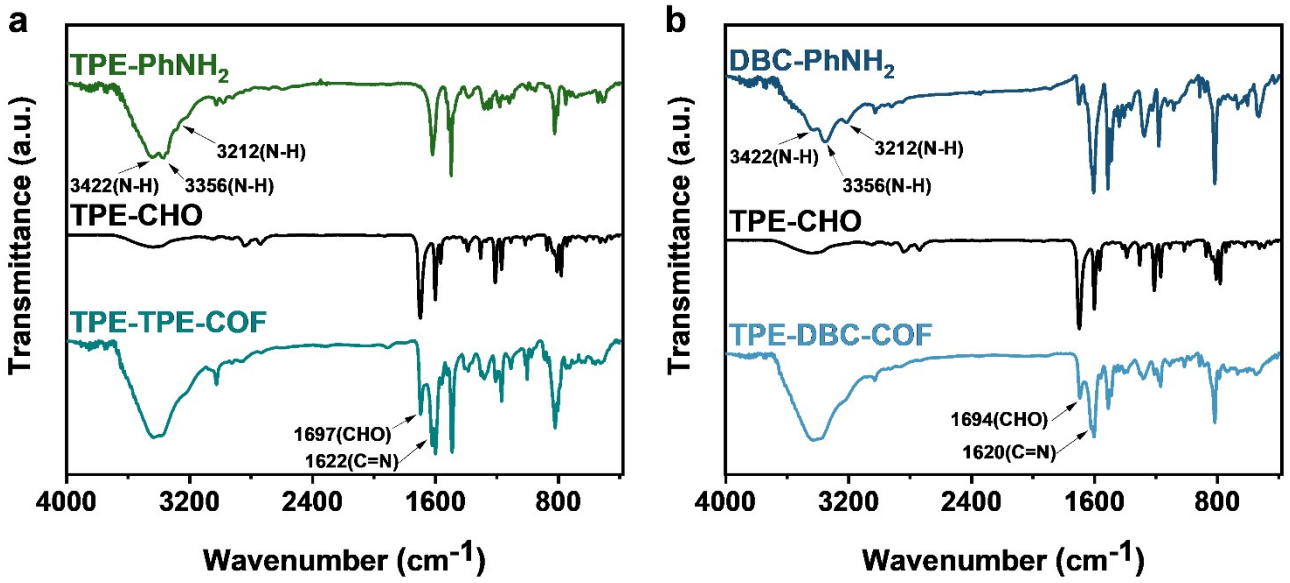

Figure S4. FT-IR spectra of (a) **TPE-TPE-COF** and (b) **TPE-DBC-COF**.

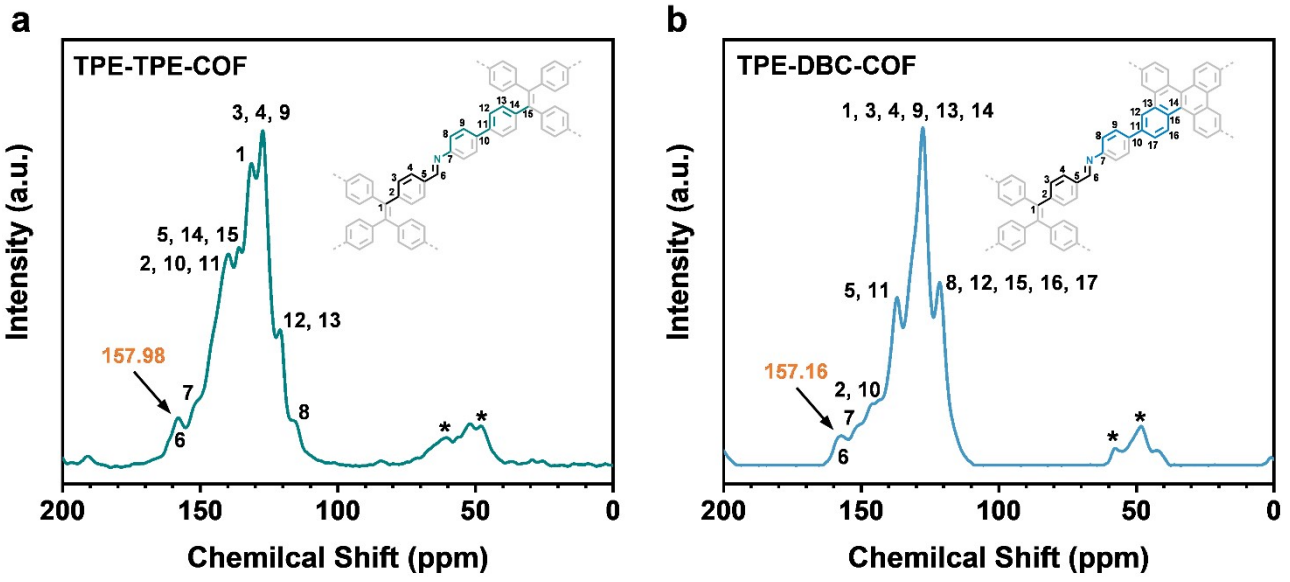

Figure S5. ^{13}C CP/MAS NMR spectra of (a) **TPE-TPE-COF** and (b) **TPE-DBC-COF**. Asterisks (*) indicate peaks may arising from solvent molecules or spinning side bands.

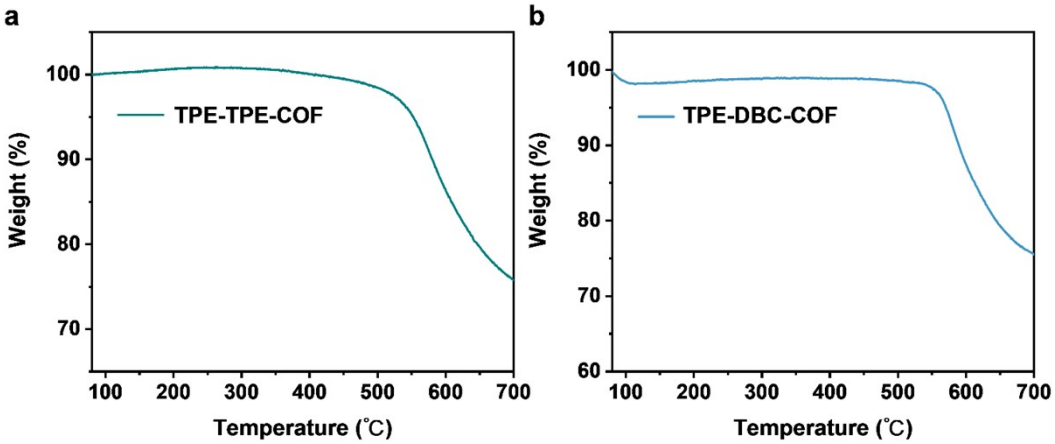

Figure S6. TGA curves of (a) **TPE-TPE-COF** and (b) **TPE-DBC-COF**.

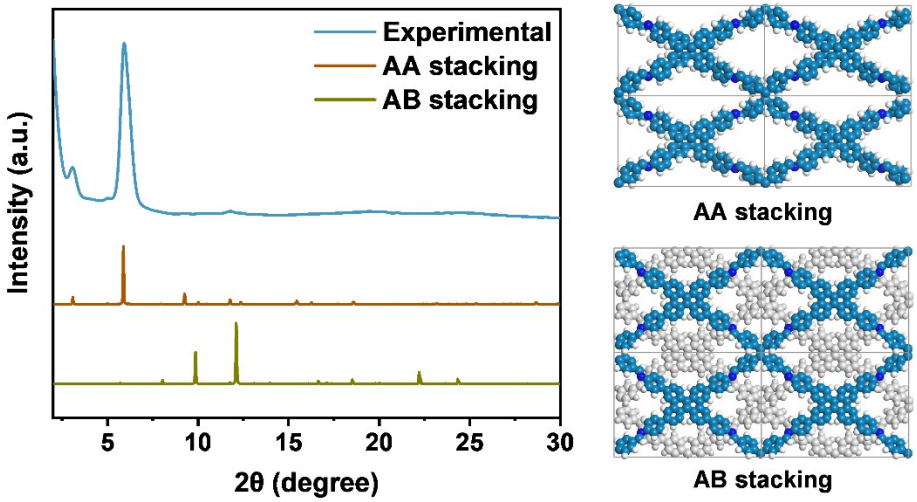

Figure S7. Simulated PXRD patterns of TPE-DCB-COF with different stacking models.

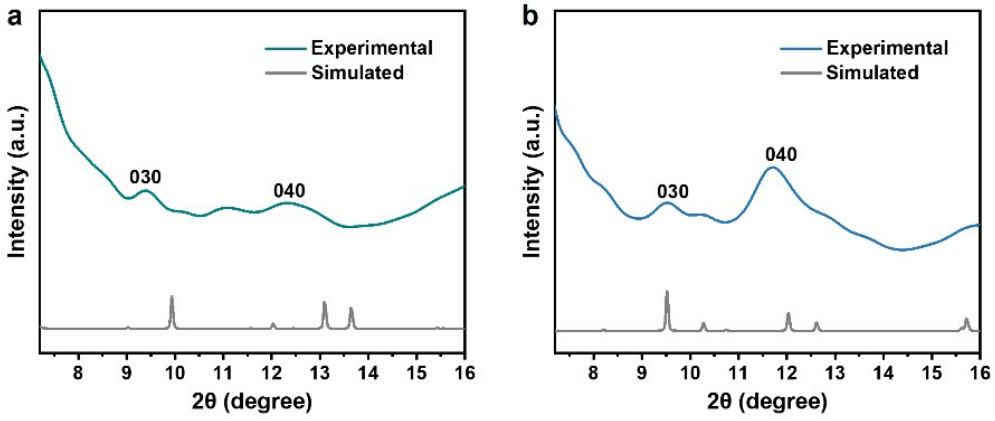

Figure S8. Enlarged experimental and simulated PXRD patterns for TPE-TPE-COF (a) and TPE-DBC-COF (b).

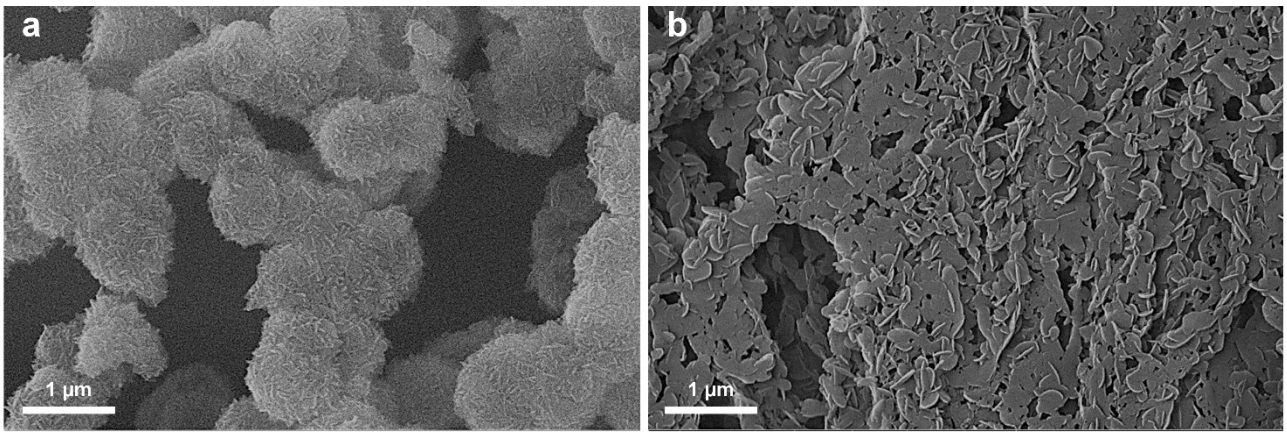

Figure S9. SEM images of (a) **TPE-TPE-COF** and (b) **TPE-DBC-COF.**

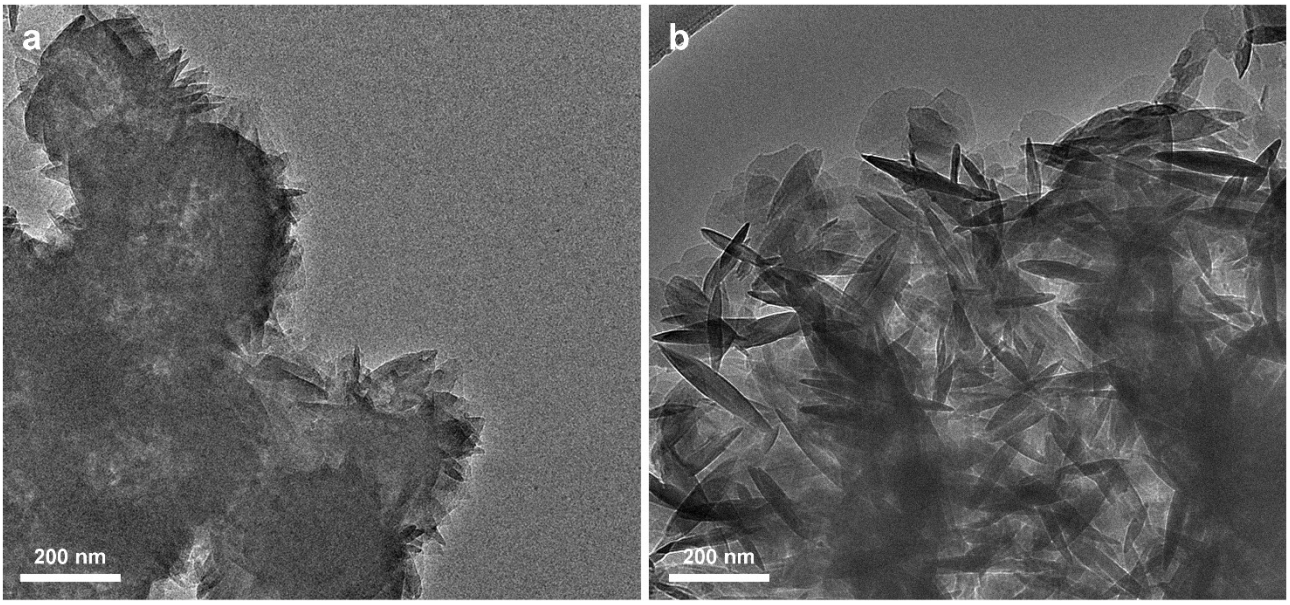

Figure S10. TEM images of (a) **TPE-TPE-COF** and (b) **TPE-DBC-COF.**

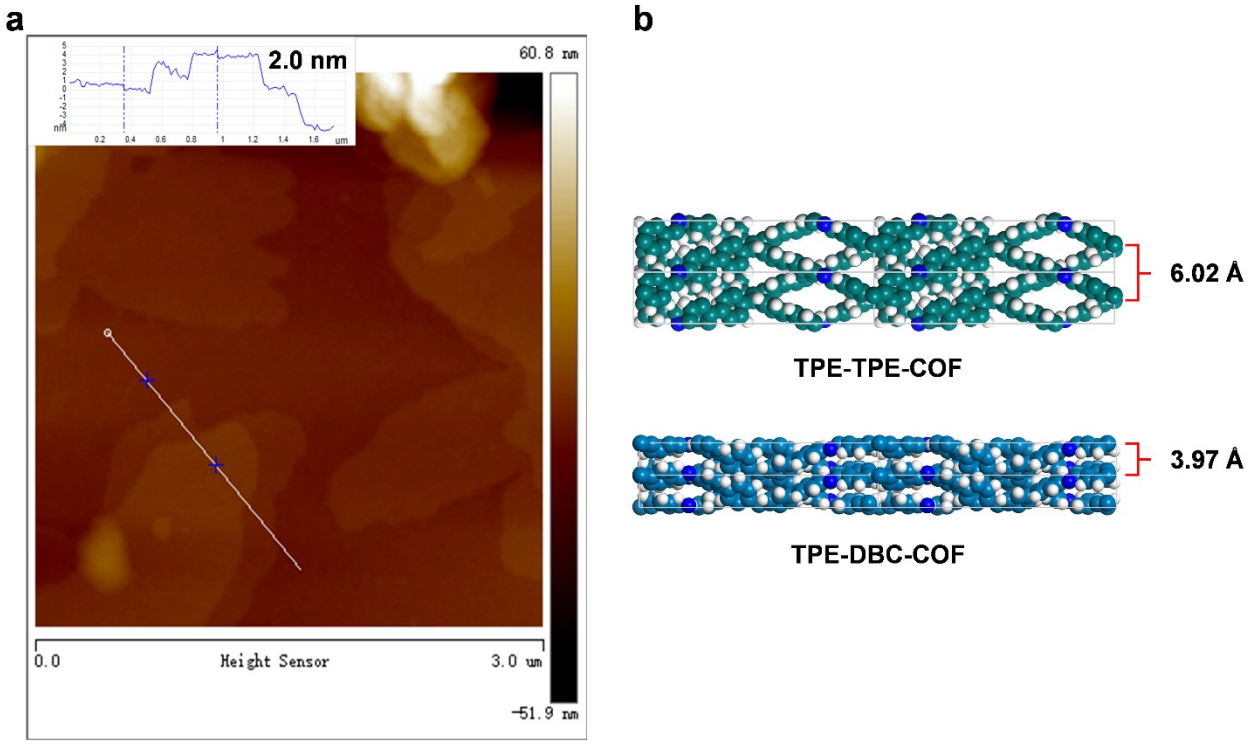

Figure S11. (a) AFM image of **TPE-DBC-COF** nanosheets with the thickness indicated. (b) Side view and layer distances of **TPE-TPE-COF** and **TPE-DBC-COF**.

2.3 Fluorescence detection performance

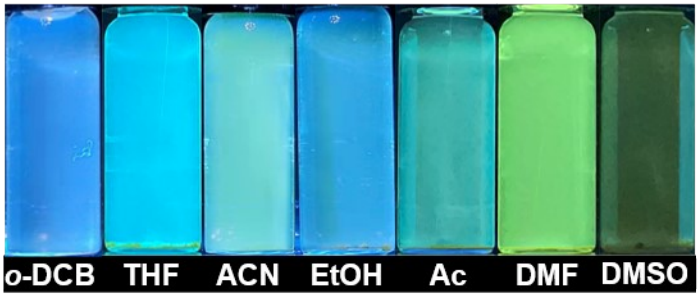

Figure S12. Photoluminescence images of **TPE-DBC-COF** dispersed in different solvents, using 365 nm illumination.

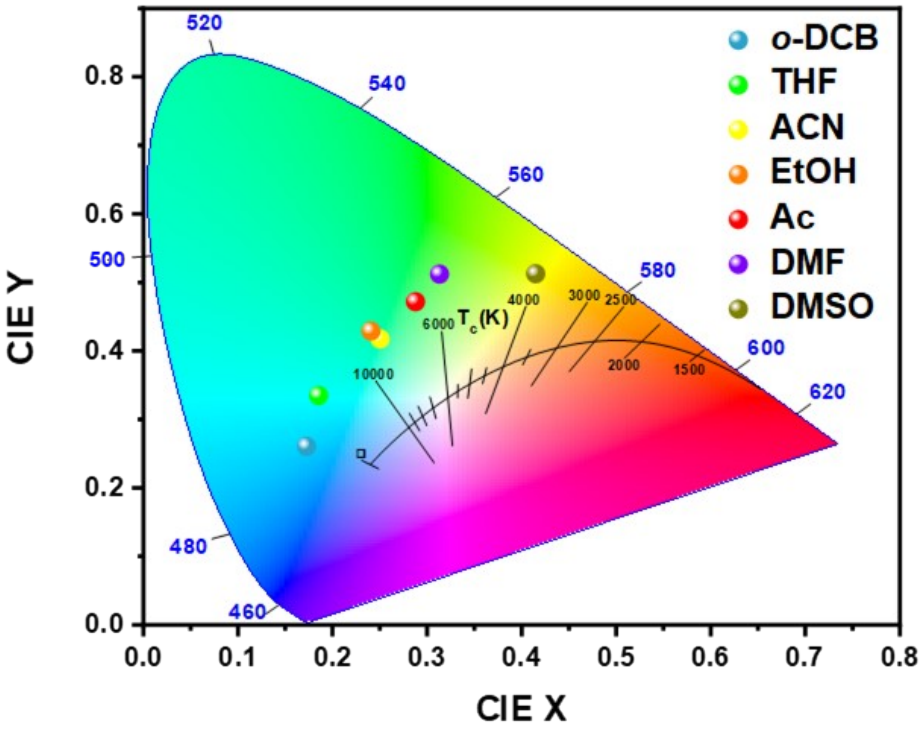

Figure S13. CIE chromaticity diagram of **TPE-DBC-COF** dispersed in different solvents, under 365 nm illumination.

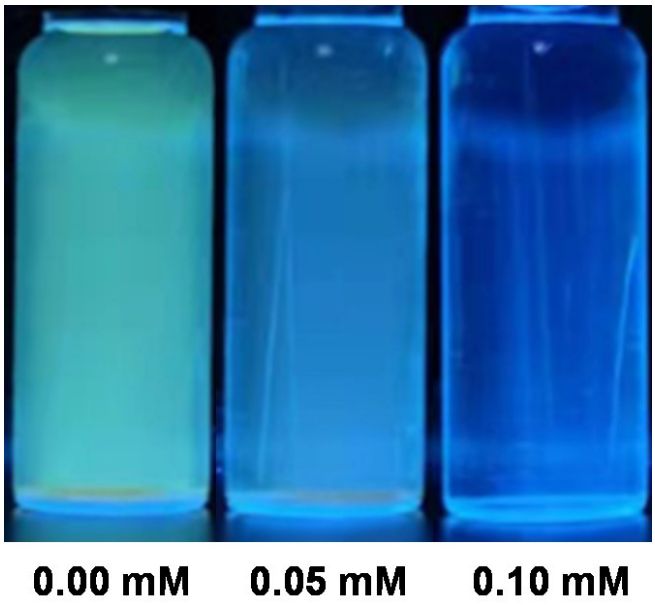

Figure S14. Fluorescence images of TPE-DBC-COF dispersed in acetone solution in the presence of different concentrations of tetracycline hydrochloride, using 365 nm illumination.

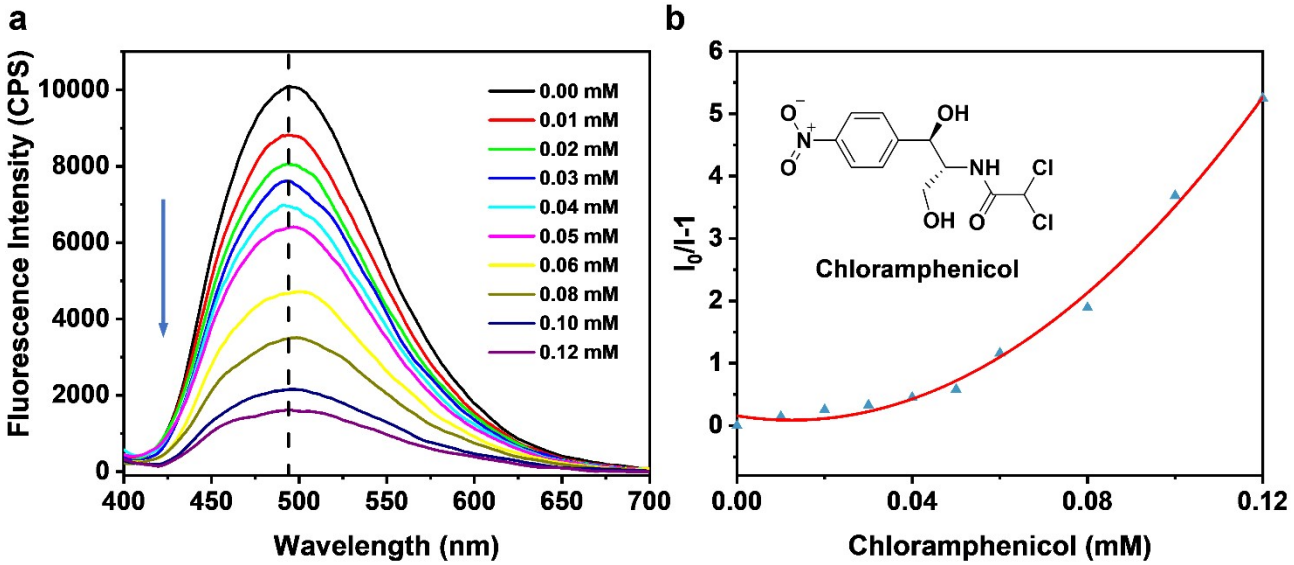

Figure S15. (a) Fluorescence quenching experiments of the **TPE-DBC-COF** upon addition of chloramphenicol (0.01-0.12 mM) in acetone. (b) Quantitative fitting curve of the fluorescence quenching process of TPE-DBC-COF nanosheets by chloramphenicol, the fitted curve is $I_0/I = 1.16 - 11.15 \times C_{chloramphenicol} + 447.54 \times C_{chloramphenicol}^2$.

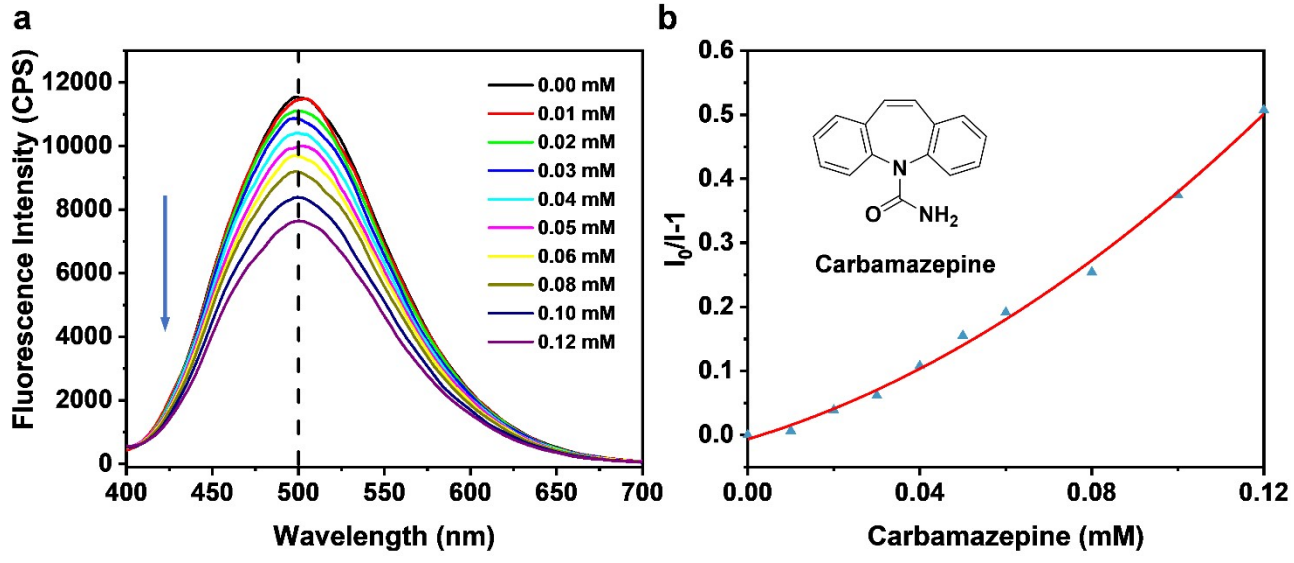

Figure S16. (a) Fluorescence quenching experiments of the **TPE-DBC-COF** upon addition of carbamazepine (0.01-0.12 mM) in acetone. (b) Quantitative fitting curve of the fluorescence quenching process of TPE-DBC-COF nanosheets by carbamazepine, the fitted curve is $I_0/I = 1.00 - 2.01 \times C_{carbamazepine} + 18.52 \times C_{carbamazepine}^2$.

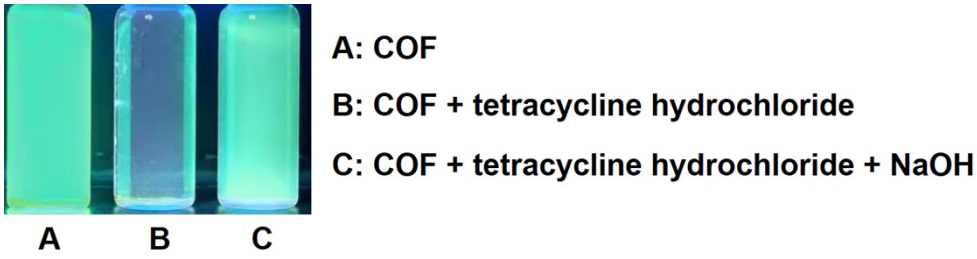

Figure S17. Fluorescence quenching images of TPE-DBC-COF by adding tetracycline hydrochloride and fluorescence recovery by adding NaOH solution.

As shown in Figure S17, in order to verify the electron transfer mechanism, the fluorescence of TPE-DBC-COF nanosheets were firstly quenched with 0.2 mM tetracycline hydrochloride, and then an equivalent of NaOH solution was added to the system. The addition of NaOH can effectively block the charge transfer process via eliminating the lack of electricity of tetracycline hydrochloride, and the fluorescence of TPE-DBC-COF nanosheets was recovered, confirming the proposed charge transfer mechanism.

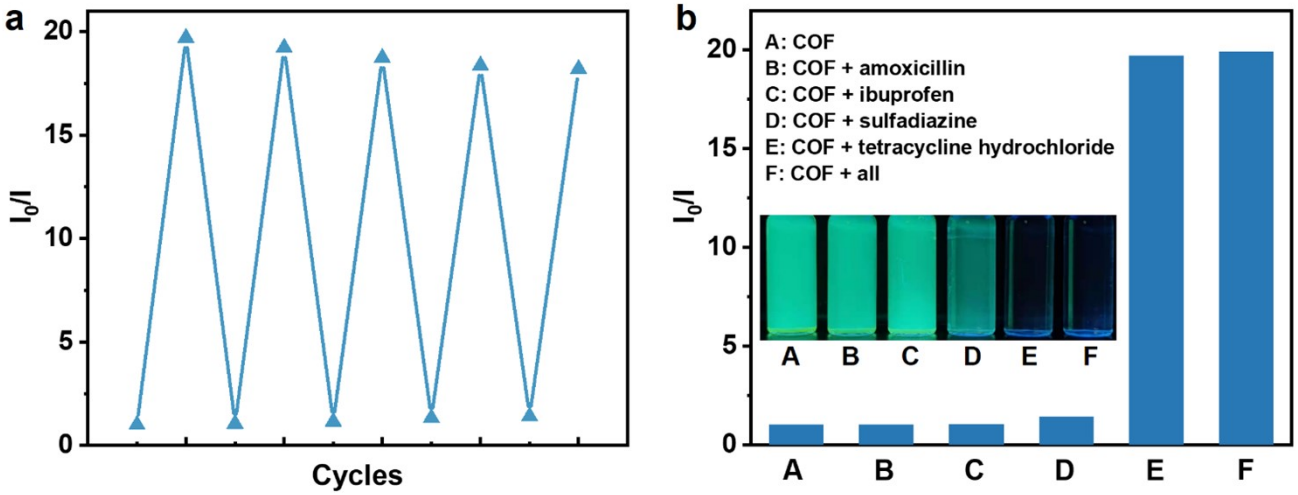

Figure S18. (a) Fluorescence quenching experiments of TPE-DBC-COF nanosheets toward 0.1 mM tetracycline hydrochloride for continuous 5 cycles. (b) Fluorescence quenching experiments of TPE-DBC-COF nanosheets upon addition of different antibiotics (0.1 mM). Inset: fluorescence quenching images. I_0 and I are the luminescence intensity of TPE-DBC-COF nanosheets before and after addition of antibiotics, using 365 nm illumination.

2.4 Unit cell parameters and fractional atomic coordinates

Table S1. Unit cell parameters and fractional atomic coordinates for **TPE-TPE-COF** calculated based on AA stacking.

Space group		*P*2	
Calculated unit cell		a = 15.3572 Å, b = 28.0463 Å, c = 6.0241 Å α = 90.0000°, β = 94.3906°, γ = 90.0000°	
Atoms	X	Y	Z
C1	0.91844	0.0464	0.61739
C2	0.96613	0.08297	0.72912
C3	0.92406	0.12421	0.79489
C4	0.83362	0.12917	0.75232
C5	0.78565	0.09266	0.64285
C6	0.82776	0.0515	0.57608
C7	0.78783	0.17163	0.82412
N8	0.82904	0.20583	0.93221
C9	0.78621	0.24763	1.00617
C10	0.83574	0.28273	1.12216
C11	0.79561	0.32387	1.19675
C12	0.70513	0.33049	1.15667
C13	0.65571	0.2951	1.04028
C14	0.69573	0.25404	0.96567
C15	0.66231	0.37421	1.23329
C16	0.57163	0.37974	1.19761
C17	0.53069	0.42121	1.26413
C18	0.57953	0.45781	1.37139
C19	0.67037	0.45253	1.40693
C20	0.7114	0.41112	1.33874
C21	0.08083	0.95674	2.38621
C22	0.10523	0.92271	2.54997
C23	0.14262	0.87953	2.49121
C24	0.15629	0.87004	2.2687
C25	0.1335	0.90434	2.10543

C26	0.09618	0.94749	2.164
C27	0.19312	0.82394	2.21022
N28	0.20528	0.81307	2.00567
C29	0.24023	0.76816	1.94246
C30	0.25249	0.7597	1.71835
C31	0.2863	0.71612	1.65213
C32	0.30824	0.68023	1.80903
C33	0.29567	0.68892	2.03378
C34	0.26196	0.73242	2.10006
C35	0.34503	0.6342	1.73984
C36	0.35889	0.62539	1.51581
C37	0.39575	0.58239	1.45253
C38	0.41981	0.54758	1.61262
C39	0.40438	0.55584	1.8354
C40	0.36753	0.59876	1.89835
C41	0.96151	0.00189	0.54911
C42	0.46221	0.50242	1.55112

Table S2. Unit cell parameters and fractional atomic coordinates for **TPE-DBC-COF** calculated based on AA stacking.

Space group		*P*2	
Calculated unit cell		a = 18.0908 Å, b = 28.6446 Å, c = 3.9676 Å α = 90.0000°, β = 77.4651°, γ = 90.0000°	
Atoms	X	Y	Z
C1	0.91339	0.03776	0.02104
C2	0.92637	0.07776	0.19648
C3	0.88696	0.11888	0.18716
C4	0.82427	0.11982	0.03556
C5	0.80385	0.07915	-0.11326
C6	0.84987	0.03959	0.86971
C7	0.77985	0.16265	0.04847
N8	0.80237	0.19869	0.19533
C9	0.76656	0.24266	0.26976

C10	0.80482	0.27586	0.42352
C11	0.77009	0.31777	0.54128
C12	0.6962	0.32706	0.503
C13	0.6587	0.29406	0.3373
C14	0.69341	0.25189	0.22318
C15	0.65717	0.37008	0.64757
C16	0.5793	0.3694	0.79083
C17	0.54061	0.41056	0.91292
C18	0.57946	0.45325	0.85712
C19	0.65917	0.45243	0.76903
C20	0.69742	0.4116	0.65355
C21	0.09153	-0.05047	-0.04488
C22	0.06946	0.90852	0.1392
C23	0.11791	0.87089	0.14142
C24	0.19258	0.8732	0.95501
C25	0.21782	0.9135	0.7723
C26	0.16867	-0.04919	0.77439
C27	0.24256	0.83275	0.92388
N28	0.21655	0.79328	1.05805
C29	0.25637	0.75039	0.98628
C30	0.33577	0.74848	0.90438
C31	0.37223	0.70763	0.76976
C32	0.32963	0.66824	0.72022
C33	0.25026	0.66984	0.81994
C34	0.21415	0.71063	0.95586
C35	0.36704	0.62533	0.56601
C36	0.43134	0.62702	0.29538
C37	0.46524	0.58566	0.14136
C38	0.432	0.5424	0.25953
C39	0.37256	0.54163	0.55253
C40	0.33891	0.58226	0.69689
C41	0.95978	-0.00709	0.01741
C42	0.46419	0.49796	0.09376

2.5 Quantum yield (PLQY) data of reported fluorescent COFs

Table S3. Comparative table for quantum yield (PLQY) data of reported fluorescent COFs

COF name	PLQY	Reference
PAF-15	14%	*J. Phys. Chem. C.*, 2012, **116**, 26431-26435
PAF-14	37.5%	*J. Mater. Chem.*, 2012, **22**, 24558-24562
Ph-An-COF	5.4%	*Angew. Chem. Int. Ed.*, 2015, **54**, 8704-8707
COF-JLU3	9.9%	*Chem. Commun.*, 2016, **52**, 6613-6616
COF-LZU8	3.5%	*J. Am. Chem. Soc.*, 2016, **138**, 3031-3037
TPE-Ph COF	32%	*J. Am. Chem. Soc.*, 2016, **138**, 5797-5800
PI-COF 201	41.6%	*New J. Chem.*, 2017, **41**, 14272-14278
PI-COF 202	38.0%	
IMDEA-COF-1	3.5%	*J. Am. Chem. Soc.*, 2018, **140**, 12922-12929
TFPPy-DETHz-COF	17%	*J. Am. Chem. Soc.*, 2018, **140**, 12374-12377
sp^2c-COF	22%	*Nat. Commun.*, 2018, **9**, 4143
sp^2c-COF-2	20%	
sp^2c-COF-3	18%	
Py-TPE-COF	21.1%	*Chem. Commun.*, 2018, **54**, 2349-2352
IISERP-COF7	64%	*J. Am. Chem. Soc.*, 2018, **140**, 13367-13374
3D-TPE-COF	20%	*Nat. Commun.*, 2018, **9**, 5234
COF-BABD-DB	54.1%	*Chem. Commun*., 2018, **54**, 2308-2311
COF-BABD-BZ	22.3%	
NUS-30	43.6%	*Chem. Mater.*, 2018, **31**, 146-160
PAF-130	29.5%	*Macromol. Rapid Commun.*, 2019, **40**, 1900060
COF-4-OH	10.7%	*Chem. Sci.*, 2019, **10**, 11103-11109
TFPPy-CHYD COF	13.6%	*ACS Sustain. Chem. Eng*., 2019, **8**, 445-451
cyano-sp^2c COF	38.1%	*Adv. Funct. Mater.*, 2020, **30**, 2000516
BCTB-PD COF	16.3%	*J. Mater. Chem. C.*, 2020, **8**, 9520-9528
BCTA-TP COF	5.6%	
BCTB–BCTA COF	21.2%	
PyTA-BC COFs	1.46%	*Adv. Opt. Mater.*, 2020, **8**, 2000641
PyTA-BC-Ph COFs	1.83%	
Eu-3D-COF	38.2%	*J. Hazard. Mater.*, 2020, **388**, 121740
iCONs	94%	*ACS Appl. Mater. Interfaces*, 2020, **12**, 13248-13255
CCOF 17-R	19.0%	*J. Am. Chem. Soc.*, 2021, **143**, 369-381
CCOF 18-R	20.5%	
COF-1	14.28%	*Dyes Pigm*., 2021, **195**, 109710
TMHzcB-DHTA-COF	3.1%	*Angew. Chem. Int. Ed.*, 2021, **60**, 2-11
TMHzcB-TFB-COF	5.1%	
TMHzcB-TFPB-COF	10.5%	

TMHzcB-TA-COF	11.7%	
TMHzcB-DCTA-COF	6%	
TMHzcB-DMeTA-COF	20%	
TMHzcB-DMeOTA-COF	19%	
TAT-COF	17.82%	*J. Am. Chem. Soc*., 2021, **143**, 1061-1068
TPB-COF	62.17%	
TPE-DHZ-COF	31.5%	*Dyes Pigm*., 2022, **204**, 110464
TPB-DHZ-COF	10.3%	
TPE-DBC-COF	**43.5%**	**This work**

3. References

(S1) Materials Studio; Accelrys: San Diego.
(S2) http://www.ba.ic.cnr.it/softwareic/expo/
(S3) http://www.jp-minerals.org/vesta/en/
(S4) Y. Liu, C. S. Diercks, Y. Ma, H. Lyu, C. Zhu, S. A. Alshmimri, S. Alshihri and O. M. Yaghi, *J. Am. Chem. Soc.*, 2019, **141**, 677-683.